Available online at www.sciencedirect.com
ScienceDirect
Journal of Sound and Vibration 315 (2008) 1003–1015
JOURNAL OF SOUND AND VIBRATION
www.elsevier.com/locate/jsvi

Eigenvalue solution for the convected wave equation in a circular soft wall duct

Jose S. Alonso*, Ricardo A. Burdisso

Virginia Tech, Vibration and Acoustics Laboratories, Durham Hall, Blacksburg, VI 24061-0238, USA

Received 31 January 2007; received in revised form 19 December 2007; accepted 6 February 2008
Handling Editor: Bolton
Available online 14 March 2008

Abstract

A numerical approach to find the eigenvalues of the wave equation applied in a circular duct with convective flow and soft wall boundary conditions is proposed. The characteristic equation is solved in the frequency domain as a function of a locally reacting acoustic impedance and the flow Mach number. In addition, the presence of the convective flow couples the solution of the eigenvalues with the axial propagation constants. The unknown eigenvalues are also related to these propagation constants by a quadratic expression that leads to two solutions. These two solutions replaced into the characteristic equation generate two separate eigenvalue problems depending on the direction of propagation. Given that the resulting nonlinear complex-valued equations do not provide the solution explicitly, a numerical technique must be used. The proposed approach is based on the minimization of the absolute value of the characteristic equation by the Nelder–Mead simplex method. The main advantage of this method is that it only uses function evaluations, rather than derivatives, and geometric reasoning. The minimization is performed starting from very low frequencies and increasing by small steps to the particular frequency of interest. The initial guess for the first frequency of calculation is provided as the hard wall eigenvalue solution. Then, the solution from the previous step is used as the initial value for the next calculation. This approach was specifically developed for applications with resonator-type liners commonly used in the commercial aviation industry, where the low-frequency behavior resembles that of a hard wall and agrees with the first initial guess for the first frequency of calculation. The numerical technique was found to be very robust in terms of convergence and stability. Also, the method provides a physical meaning for each eigenvalue since the variation as a function of frequency can be clearly followed with respect to the values that are originally linked to the hard wall modes.
© 2008 Elsevier Ltd. All rights reserved.

1. Introduction

The analytical treatment of sound propagation inside circular lined ducts with uniform flow has been extensively investigated as a design and optimization tool for the acoustic liners typically used for noise control of turbofan engines. The first studies consisted in deriving the equations of acoustic motion inside ducts with different cross-section shapes and general mean flow distributions [1,2]. In addition, the appropriate soft wall boundary condition was also introduced in order to correctly account for the interaction

*Corresponding author.
E-mail address: jalonsom@vt.edu (J.S. Alonso).

0022-460X/$ - see front matter © 2008 Elsevier Ltd. All rights reserved.
doi:10.1016/j.jsv.2008.02.006

Nomenclature

a	duct radius
A	modal amplitude
c	speed of sound
i	imaginary unit, $i^2 = -1$
k	wavenumber, eigenvalue
M	Mach number
p	acoustic pressure
r	spatial coordinate (radial)
t	time
v	particle velocity
z	spatial coordinate (axial)
β	specific acoustic admittance
θ	spatial coordinate (angular)
Φ	acoustic mode
ω	angular frequency

Subscripts and superscripts

ℓ, $+$, $-$	direction of propagation
m	circumferential mode order
n	radial mode order
w	wall

between the grazing flow and the impedance wall. This boundary condition was first developed for rectangular [3,4] and circular [5] ducts using continuity of pressure and particle displacement. Later, a more formal analysis was stated by Myers [6] for a duct of arbitrary shape and flow field. Nevertheless, both approaches lead to the same formulation for ducts with constant cross-section and uniform flow parallel to the duct axis. The effects of shear flows in the regions close to the duct walls were also subject of extensive investigation. The main concern of these studies was focused on how the boundary layer profile affects the uniform flow assumption on the derivation of the boundary condition. It was determined that provided that the boundary layer is thin enough, the shear flow effects can be properly accounted for in a model for the wall impedance while the flow distribution can still be assumed uniform [7].

This paper is related to the application of a numerical method to find modal solutions for the particular case of a lined duct with constant circular cross-section, uniform mean flow parallel to the duct axis, and locally reacting wall impedance. Under these assumptions, the eigenvalue problem is reduced to finding the roots of a single transcendental characteristic equation in the frequency domain that depends on the wall normalized impedance and the flow Mach number. However, the presence of the flow couples the eigenvalue solutions with the axial propagation constants for the corresponding modes. Since the relation between these two parameters is quadratic, the original characteristic equation splits into two branches depending on the direction of sound propagation. Solving the resulting two transcendental equations using typical root-finding numerical methods can be quite inefficient or unstable since the solutions must be found in the complex plane rather than the real axis. In contrast, the method adopted in this investigation is based in minimizing the absolute value of the characteristic equations using the Nelder–Mead simplex method. This method was developed for minimization of a (nonlinear) scalar function of multiple variables only using function evaluations, rather than derivatives, and geometric reasoning. In each step, the function is evaluated at the vertices of a *simplex* (a generalized triangle in multiple dimensions), which is then deformed towards the function minimum. For this application, the scalar function is defined as the absolute value of the soft wall characteristic equation and the two variables are the real and imaginary parts of the complex-valued eigenvalues. Given that the characteristic equation itself must equal zero at the eigenvalue solutions, each minimum is also expected to approach zero and be located at the roots of the equation (eigenvalues). For the first step of calculation, an initial guess must be provided as the centroid of the first simplex. The computed complex-valued eigenvalues are finally replaced into the system eigenfunctions in order to represent the modes inside the lined circular duct. The approach can be easily extended to other duct geometries that allow closed-form solutions for the duct modes.

2. Analytical modeling

The propagation of sound inside the lined circular duct with flow is described by the homogeneous solution to the acoustic wave equation in a moving medium [1]. For the case considered in this paper, the duct is

assumed to be infinitely long in the axial z-direction and embedded in a liner with locally reacting impedance. The flow is assumed to be constant along the duct axis and uniform across the cross section. Fig. 1 presents a schematic of the assumed geometry and the cylindrical coordinate system. Under these assumptions and considering harmonic motion of the form $e^{i\omega t}$, the convected wave equation can be expressed in terms of the acoustic pressure as

$$\frac{\partial^2 p}{\partial r^2}+\frac{1}{r}\frac{\partial p}{\partial r}+\frac{1}{r^2}\frac{\partial^2 p}{\partial \theta^2}+\frac{\partial^2 p}{\partial z^2}=-k_0^2 p+2iMk_0\frac{\partial p}{\partial z}+M^2\frac{\partial^2 p}{\partial z^2}, \tag{1}$$

where k_0 is the acoustic free wavenumber and M is the flow Mach number. The solution to Eq. (1) is expressed in the frequency domain as a linear superposition of the propagating modes inside the lined circular duct as

$$p_\omega(\vec{r})=\sum_{m=0}^{M}\sum_{n=0}^{N}A_{mn}^{(+)}\Phi_{mn}^{(+)}(r,\theta)\,e^{-ik_z^{(+)}z}+\sum_{m=0}^{M}\sum_{n=0}^{N}A_{mn}^{(-)}\Phi_{mn}^{(-)}(r,\theta)\,e^{-ik_z^{(-)}z}, \tag{2}$$

where the superscripts $(+)$ and $(-)$ indicate variables associated to positive and negative z-direction propagation and the subscripts m and n refer to the circumferential and radial mode order, respectively. For the circular duct geometry, the acoustic modes are found in terms of spinning exponential functions in the circumferential direction and Bessel functions of the first kind in the radial direction as [8–10]

$$\Phi_{mn}(r,\theta)=A_{mn}e^{\pm im\theta}J_m(k_{mn}r),\quad m=0,1,2,3,\ldots,\quad n=0,1,2,3,\ldots, \tag{3}$$

where A_{mn} is a complex-valued modal amplitude and the argument k_{mn} is the mode eigenvalue. The solution in Eq. (3) is completely defined by finding the correct eigenvalue k_{mn} from the characteristic equation that represents the soft wall boundary condition. In addition, the axial wavenumbers k_z are also associated with every mode and are found from the following quadratic dispersion relationship as

$$k_{mn}^2=k_0^2-k_z^2(1-M^2)-2k_0k_zM. \tag{4}$$

The characteristic equation is obtained by applying the equilibrium Euler's equation in the radial direction at the duct wall in combination with the soft wall boundary condition, including the effect of the flow [3–6], given in terms of the wall specific acoustic admittance β_w. Using the pressure solution in Eqs. (2) and (3), this equation can be found as

$$i\beta_w\frac{(k_0-Mk_z)^2}{k_0}J_m(k_{mn}a)=-k_{mn}J_m'(k_{mn}a). \tag{5}$$

One of the difficulties in solving Eq. (5) arises because the flow Mach number produces a coupling of the eigenvalue solutions k_{mn} with the particular value of the axial wavenumbers k_z that are obtained from the quadratic expression in Eq. (4). Therefore, the wavenumbers k_z are not simply obtained from the eigenvalues but they also influence the final solution k_{mn}. Given that the relation in Eq. (4) is quadratic, the characteristic equation then breaks into two branches that are associated with each solution k_z of the quadratic relation, which also represent a direction of propagation, i.e. $k_{mn}^{(+)}$ and $k_{mn}^{(-)}$ for positive and negative propagation,

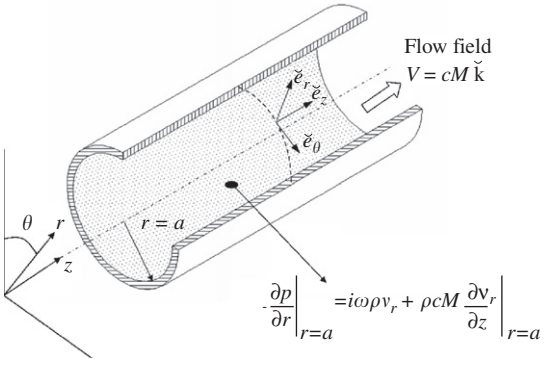

Fig. 1. Schematic of the assumed infinite circular duct with soft wall and uniform flow in the cylindrical coordinate system.

respectively. This leads to find two sets of eigenvalues, $k_{mn}^{(+)}$ and $k_{mn}^{(-)}$, also for each direction of propagation, meaning that the mode shapes inside the duct also depend on the propagation side (contrary to the hard wall case). The characteristic equations for each solution branch can be expressed as

$$k_{mn}^{(+)}J'_m(k_{mn}^{(+)}a) + \mathrm{i}\beta_w \frac{(k_0 - Mk_z^{(+)})^2}{k_0} J_m(k_{mn}^{(+)}a) = 0, \tag{6a}$$

for positive propagation, and

$$k_{mn}^{(-)}J'_m(k_{mn}^{(-)}a) + \mathrm{i}\beta_w \frac{(k_0 - Mk_z^{(-)})^2}{k_0} J_m(k_{mn}^{(-)}a) = 0 \tag{6b}$$

for the negative direction. The two axial wavenumbers k_z that follow from Eq. (4) are assigned as

$$k_z^{(+)} = \frac{-k_0 M + \sqrt{k_0^2 - (1-M^2)k_{mn}^2}}{(1-M^2)},$$
$$k_z^{(-)} = \frac{-k_0 M - \sqrt{k_0^2 - (1-M^2)k_{mn}^2}}{(1-M^2)}. \tag{7}$$

The particular selection of the complex-valued square root sign in order to satisfy the positive and negative propagation direction convention defined in Eq. (7) will be discussed in the next section, where the numerical solution is investigated.

3. Numerical approach to solve eigenvalues

Despite having a closed-form expression for the circular duct modes, the eigenvalues k_{mn} required to compute the solution must be solved numerically from the derived characteristic equation. As derived in the previous section, this equation is complex-valued, frequency dependent, nonlinear with respect to the eigenvalues, and has two solution branches that are associated with the direction of propagation. In addition, the eigenvalues are also complex-valued and must be computed in the appropriate sequence in order to avoid skipping any mode order. For these reasons, typical root-finding numerical methods can be quite inefficient to find the eigenvalues, or even unstable for certain modes. The main objective of this paper is to provide an alternative numerical approach to solve this problem based on the minimization of the absolute value of the characteristic equation. The minimization is performed using the Nelder–Mead simplex method and requires knowledge of an initial guess close to the desired eigenvalue. The general steps of the approach are described next in addition to the appropriate function definitions corresponding to the problem stated in Eq. (6).

3.1. Nelder–Mead simplex method

The Nelder–Mead simplex method was developed to minimize a scalar real-valued nonlinear function of multiple real variables and without constraints [11,12]. In the case of mathematically involved functions, the advantage of this method is that it only uses function evaluations, rather than derivatives, and geometric reasoning. To this end, the concept of a *simplex*, a generalized triangle in n dimensions, is used. In every iteration, the function to be minimized is evaluated at the $n+1$ vertices of the starting simplex; so they can be ordered as $x_1, x_2, \ldots, x_{n+1}$ such that $f(x_1) \leqslant f(x_2) \leqslant \cdots \leqslant f(x_{n+1})$. The vertex x_1 is classified as the best point, and x_{n+1} as the worst point of the simplex. Then, a series of geometric operations are applied to the simplex with the objective of obtaining new improved vertices and eliminating the worst points from the initial ordering. These operations are reflection, contraction, expansion and shrinkage [12] with respect to a reference point $\overline{x}$. Fig. 2 presents a schematic of these operations on a two-dimensional simplex (triangle).

Once the set of improved simplexes is obtained, the function is evaluated at the new vertices in order to determine which ones will replace the worst points from the previous iteration. Finally, the best points will be stored to form the new simplex that will be used as the starting point of the next iteration (see Refs. [11,12] for

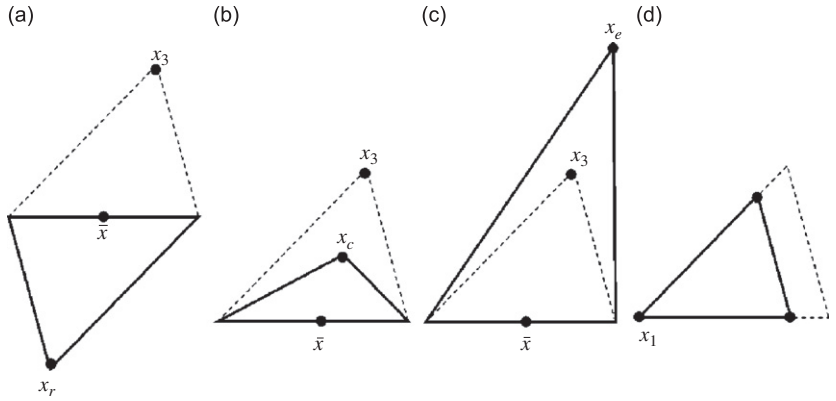

Fig. 2. Application of the basic deforming operations of: (a) reflection, (b) contraction, (c) expansion and (d) shrinkage. The original simplex is shown by the dashed line.

details about the method). The process is repeated until the minimum is reached to within a certain precision imposed by the user.

The Nelder–Mead simplex method has become very popular as a minimization algorithm for nonlinear equations. In fact, it has been introduced into the built-in numerical libraries of several programming languages as Fortran, C, and MATLAB [13–15]. For this reason, it is not intended to provide a more detailed description of the method other than the remark that its implementation could be relatively simple in a computer application.

3.2. Function definition

In order to apply the Nelder–Mead simplex method, the real-valued function to be minimized is defined as the absolute value of the characteristic equations in Eq. (6) derived for both directions of propagation. Since the characteristic equation itself must equal zero at the eigenvalue solutions, the defined absolute value function will also vanish at the location of its minimum values, which correspond to the roots of the equation. Then, the nonlinear functions to be minimized are defined as

$$f^{(+)} = \left| k_{mn}^{(+)} J'_m(k_{mn}^{(+)} a) + \mathrm{i}\beta_w \frac{(k_0 - k_z^{(+)} M)^2}{k_0} J_m(k_{mn}^{(+)} a) \right|,$$
$$f^{(-)} = \left| k_{mn}^{(-)} J'_m(k_{mn}^{(-)} a) + \mathrm{i}\beta_w \frac{(k_0 - k_z^{(-)} M)^2}{k_0} J_m(k_{mn}^{(-)} a) \right|. \quad (8)$$

In addition, note that the simplex method is intended only for expressions that are a function of multiple real-valued variables. For this reason, the unknown complex-valued eigenvalues are also rearranged by separating their real and imaginary components in two independent real-valued variables as

$$k_{mn}^{(+)} = \mathrm{Re}[k_{mn}^{(+)}] + \mathrm{i}\,\mathrm{Im}[k_{mn}^{(+)}] = X^{(+)} + \mathrm{i}\,Y^{(+)},$$
$$k_{mn}^{(-)} = \mathrm{Re}[k_{mn}^{(-)}] + \mathrm{i}\,\mathrm{Im}[k_{mn}^{(-)}] = X^{(-)} + \mathrm{i}\,Y^{(-)}. \quad (9)$$

In conclusion, the real-valued functions defined in Eq. (8) are minimized in terms of the two independent unknowns, i.e. X and Y, and the eigenvalues are later computed by using Eq. (9). As mentioned before, the algorithm must be provided with an approximate initial guess for each root to be searched. In order to obtain the correct mode ordering sequence, the approach taken consists in starting the computation from very low frequencies and advancing by very small steps up to the desired frequency of calculation. For resonator-type liners, this approach allows using the hard wall eigenvalues as the initial guess for the first step since the reactance at the lower frequencies approaches (negative) infinite values, i.e. the liner behaves as a hard wall. Then, the result obtained for each step is used as the initial guess for the next point of calculation and up to the

desired frequency. Note that after the whole process is finished, it is possible to identify the tracking of the eigenvalues $k_{mn}^{(+)}$ and k_{mn}^{-} on the complex plane as a function of frequency and, therefore, identify the proper mode order based on the hard wall condition.

It is important to also remark that although this application is mainly concentrated on the circular duct geometry, the presented approach can be easily extended to other cross-section geometries that also have closed-form solutions and lead to similar characteristic equations, e.g. annular, elliptical or rectangular ducts. In fact, the only difference is reflected in a re-definition of the functions to be minimized in Eq. (8).

3.3. Solution branches

The two solution branches of the characteristic equation are associated with the propagating direction along the duct axis. As previously shown, these branches appear as a consequence of the quadratic relation between the eigenvalues k_{mn} and the axial wavenumber k_z, which directly affects the impedance term in Eq. (8). The parameter controlling each side of the solution is the sign of the square root in the expression for the axial wavenumbers $k_z^{(+)}$ and $k_z^{(-)}$ (see Eq. (7)). For the analyzed soft wall case, the selection of this sign must be done carefully since the square root term is always complex valued and could lead to confusion depending on the quadrant location in the complex plane. In the hard wall case, this problem is not present since the eigenvalues k_{mn} are real valued and indistinct for both propagating directions. Thus, the square root terms in Eq. (7) are either purely real or purely imaginary, indicating that the mode is either propagating (cut-on) or decaying (cut-off), respectively [16]. In this case, it is simple to recognize the direction of propagation of the particular mode by looking at the sign of the square root term, which represents the phase speed with respect to the flow when real and the direction of decay when purely imaginary. However, a more detailed analysis must be carried out for the soft wall case in order to: (a) keep the two individual branches separated and (b) assign the proper direction of propagation to each eigenvalue. To keep the two branches separated during the calculation, special care must be taken with the sign of the complex-valued square root that is provided by the numerical solver. Typically, only one of the two solutions is provided and constrained to a certain semi-plane in the complex domain, which may not correspond to the solution branch in consideration. It is important to remark that, once the two branches are separated, one of the two solutions of the square root has to be discarded and cannot be used for the other branch (because there will be a whole separate computation for the other branch). In other words, the same square root sign has to be consistently selected throughout the whole calculation in order to avoid jumping to the wrong solution within a single branch. For this reason, the solver may have to be manually forced to provide the correct sign that corresponds to the appropriate quadrant. Regarding the direction of propagation, the problem is certainly more complicated than simply looking at the decay direction of the modes since the possibility of unstable solutions when mean flow is present in a lined duct has been previously identified [4]. These unstable solutions were investigated in detail by Rienstra [17] and were identified to represent surface waves meaning that the corresponding mode is spatially confined to the immediate neighborhood of the wall. A strict causality analysis suggested that these solutions could be representing spatial instabilities for certain combinations of impedance and Mach numbers, and they might be associated with the unstable nature of the wall shear layer that separates the flow from the liner cavity. Several other references [18–22] recognize the possibility of spatial instabilities but their existence is still very much an open question because there is no experimental evidence of spatial amplification on real lined ducts. In fact, some investigators solving the mode propagation in finite length liners never mentioned the possibility of any unstable mode [9,23,24]. A study presented by Koch and Möhring [25] remarks that the presence of instabilities may be compensated by other nonlinearities which are, in fact, not modeled. Thus, these instabilities may be disregarded in order to obtain a first approximation using a linear model. Based on this discussion, this work will not consider the possibility of instabilities and all modes will be assumed to decay in the directions they propagate. However, if a particular application requires the identification of possible instabilities, the method adopted here can still be adjusted (relatively simply) for this purpose, provided it is based on tracking the eigenvalues from the hard wall condition. A brief discussion on this subject will be presented in the next subsection. For the decaying-mode condition, the imaginary part of k_z must be selected as negative for modes propagating in the positive direction and positive for the negative direction. But as mentioned before, it is also required to carefully control the sign of the square root term in Eq. (7) in order to

obtain the correct value for k_z and avoid the solution to jump to different branches due to the numerical solver. The convention adopted here consists in always computing the square root in the negative complex semi-plane, i.e. $\mathrm{Im}\left[\sqrt{k_0^2-(1-M^2)k_{mn}^2}\right]<0$, and directly replacing this root in the expressions in Eq. (7) with the + or − sign manually assigned. Then, the wavenumbers $k_z^{(+)}$ and $k_z^{(-)}$ as defined in Eq. (7) will ensure positive and negative propagation, respectively, as long as the same solution branch is used throughout the whole calculation. Also, the eigenvalues $k_{mn}^{(+)}$ and $k_{mn}^{(-)}$ will correspond with the same wavenumbers, i.e. $k_z^{(+)}$ and $k_z^{(-)}$, and apply to the positive and negative propagating modes, respectively.

3.4. Advantages of tracking the eigenvalues in frequency

As described above, the solution procedure consists in tracking the eigenvalues by small steps in frequency and starting from very low frequencies where the impedance is assumed to be infinity. Then, the computation continues by slowly increasing the frequency and adjusting the impedance according to a certain impedance law. For the application considered in this paper, this is very suitable for resonator-type liners, typically used for aero-engines, and allows investigating how the attenuation properties of a particular liner behave as a function of frequency. But since the eigenvalues are being tracked by small steps, the method also provides flexibility to follow arbitrary impedance laws or ideal contours in order to analyze other, more fundamental problems such as identifying surface waves and performing causality analysis. The key for a correct solution is to always trace the solution and start from a known initial value. A detailed discussion on how to approach this fundamental analysis, which is also based on tracing the eigenvalues from the hard wall condition, has been provided by Rienstra [17].

Another implication of this concept of tracking the eigenvalues in frequency is related to solution of the double-pole type. These solutions occur when the eigenvalues of two different modes of the same circumferential order approach the same complex value. In the vicinity of these points, any irregularities can be clearly detected by following the solution through its individual path and inspecting if the eigenvalue jumped to the incorrect trajectory after reaching the double pole. But the fact that the solution is started from two separate points guarantees that no mode orders will be skipped in the calculation in the case that a double point is reached. Also, since the two eigenvalues are expected to follow two individual paths (with frequency), a simple inspection of the results will make evident if the two solutions have merged after the double point. Re-adjusting the step size of the numerical routine to a smaller value usually is enough to avoid this problem. A second alternative is to compute the eigenvalues up to the double-pole point, and then obtain the rest of the trajectory by starting from the other frequency end (that corresponds to the liner anti-resonance) and descending in frequency down to the double pole. A brief comment to clarify this point will be provided later in the numerical results.

4. Numerical results

As an illustration of the proposed numerical approach, the mode eigenvalues k_{mn} and wavenumbers k_z are solved for a particular lined duct configuration with uniform flow. As described in the previous sections, the inputs required are the hard wall eigenvalues (initial guess for the first step), the fluid properties, the flow Mach number, and the liner normalized impedance (or admittance). The considered normalized impedance corresponds to a resonator-type liner and it is defined as

$$\frac{Z_w}{\rho c}=R+\mathrm{i}\left(mf-\cot\left(\frac{2\pi f}{c}\,\mathrm{d}\right)\right), \tag{10}$$

where $R=1.5$, ρc is the liner resistance, $m=5.0\mathrm{E}{-5}\,\mathrm{s}$ is the facing screen reactance slope, $d=2.54\,\mathrm{cm}$ is the liner core depth, and f is the frequency in Hz. The investigated frequency range is from 0 to 6750 Hz, i.e. anti-resonance of the liner, in small increments of 5 Hz. The density and speed of sound of the fluid are assumed as $\rho=1.21\,\mathrm{kg/m^3}$ and $c=343\,\mathrm{m/s}$, respectively. The radius of the infinite duct is $a=50\,\mathrm{cm}$ and the simulated

flow conditions are defined by the Mach numbers $M = 0.0$, -0.2, and -0.4, i.e. the flow direction is opposite to the positive sound propagation. The results are presented in the following subsections.

4.1. Eigenvalues

The obtained complex-valued (non-dimensional) mode eigenvalues ak_{mn} are presented in Figs. 3–5 for the flow conditions $M = 0.0$, -0.2 and -0.4, respectively. The curves in these figures represent the evolution of each eigenvalue on the complex plane as a function of frequency. The arrows indicate the direction of evolution for increasing frequency. For simplicity, only the first three circumferential orders, i.e. $m = 0$, 1, and 2, are shown since higher orders follow similar behavior. In addition, the results for 10 radial modes are presented for each circumferential order. Note that for the case without flow, i.e. $M = 0.0$, the eigenvalues for positive and negative propagating direction are indistinct (Fig. 3). In contrast, the cases with flow do not reproduce this symmetry and the eigenvalues describe different paths depending on either direction of propagation (Figs. 4 and 5). Regardless of the flow condition, it is observed that the eigenvalues start displacing from the hard wall values at very low frequencies and return to these values at the highest frequency corresponding to the anti-resonance of the liner. This result is expected since the liner behaves virtually as a rigid boundary for the two limit frequencies, i.e. impedance approaches infinity. Additionally, the first radial order describes a significantly wider path than the rest of the modes and eventually encloses a few of them. Except for these enclosed modes (including the first radial order), the path described by higher order modes is a closed trajectory that ends on the same "hard wall" order as the starting point. However, the trajectory of the first radial order ultimately approaches the hard wall eigenvalue of the last enclosed order. Subsequently,

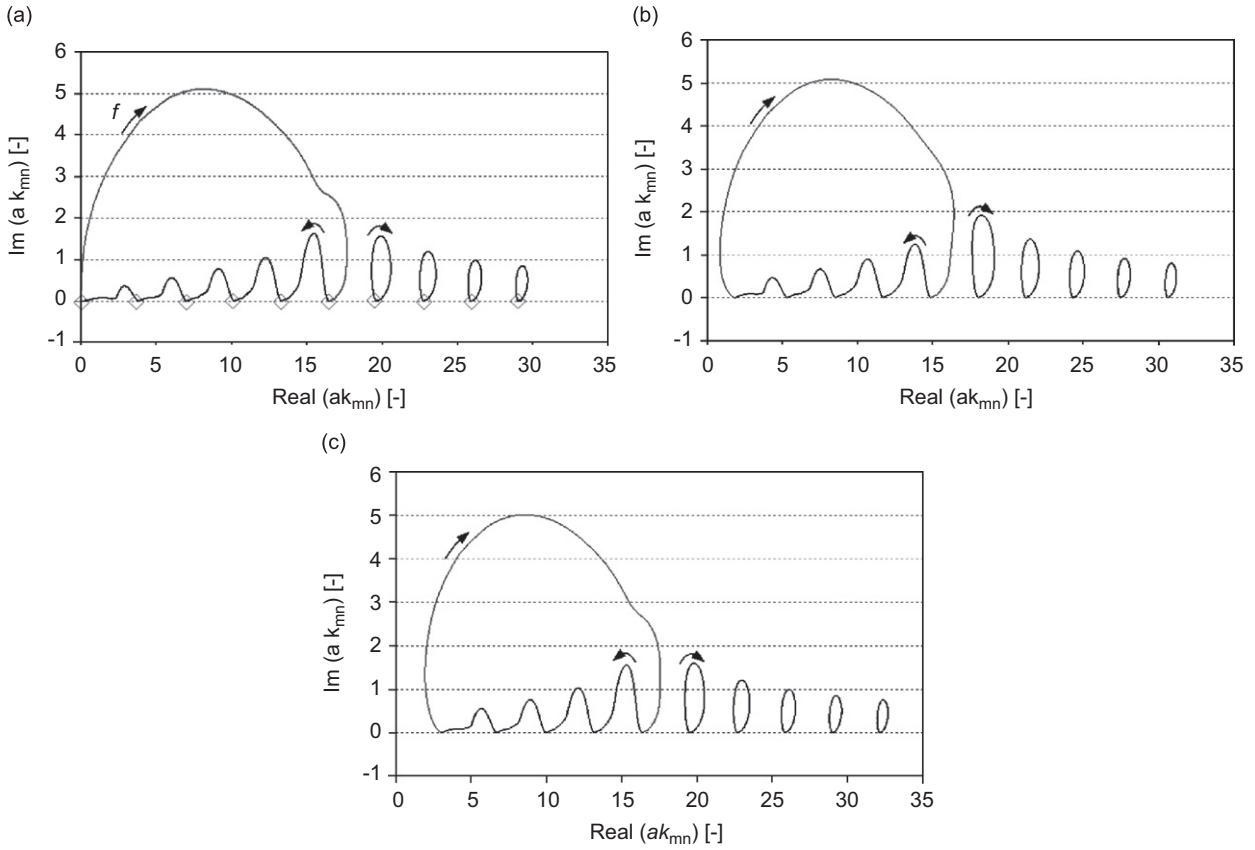

Fig. 3. Evolution of the non-dimensional eigenvalues in the complex plane for the circumferential mode orders: (a) $m = 0$, (b) $m = 1$ and (c) $m = 2$, for the case without convective flow ($M = 0.0$) and using the impedance law in Eq. (24). Key: ($\diamond$) hard wall eigenvalues; (——) positive and negative propagation eigenvalues ($k_{mn}^{(+)} = k_{mn}^{(-)}$).

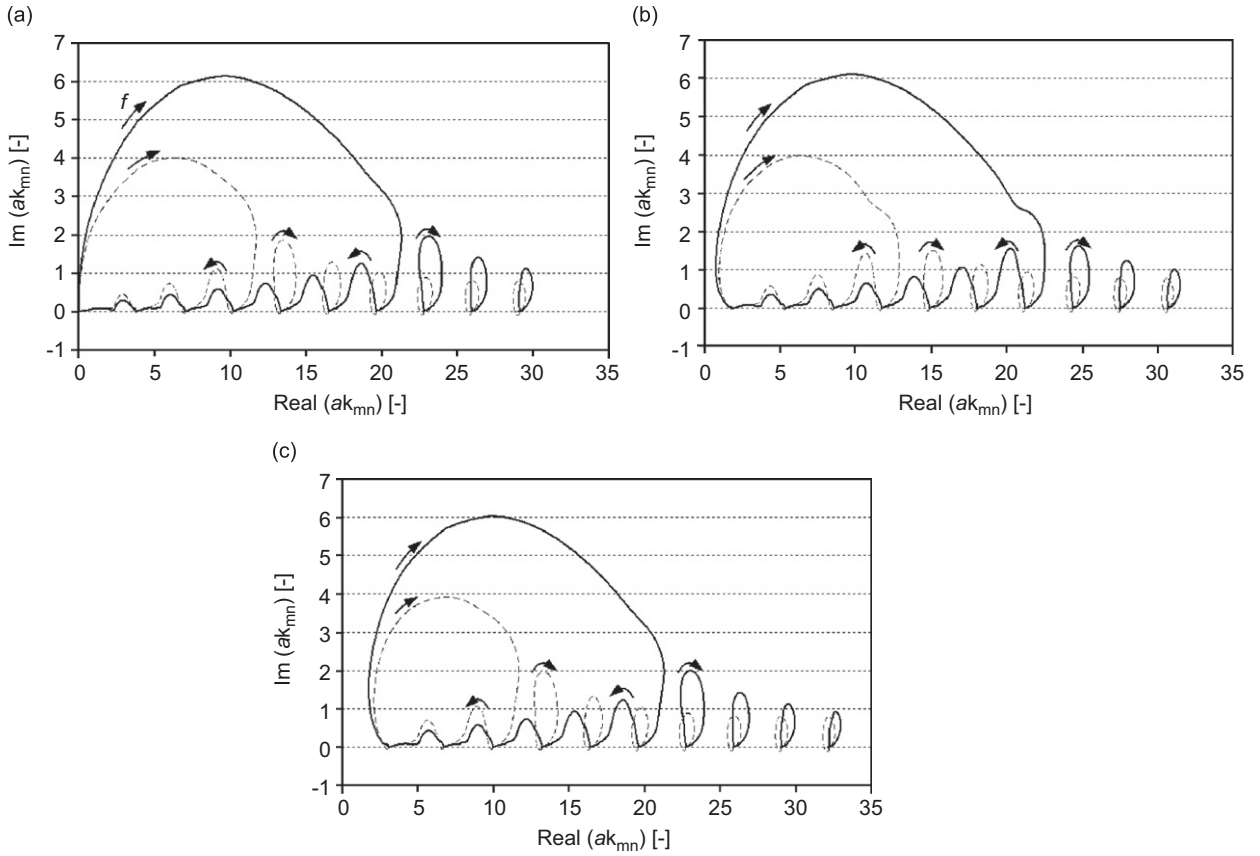

Fig. 4. Evolution of the non-dimensional eigenvalues in the complex plane for the circumferential mode orders: (a) $m = 0$, (b) $m = 1$ and (c) $m = 2$, including convective flow $M = -0.2$ and using the impedance law in Eq. (24). Key: (——) positive propagation eigenvalues $k_{mn}^{(+)}$; and (- - - - -) negative propagation eigenvalues $k_{mn}^{(-)}$.

each of the enclosed modes approaches the hard wall eigenvalue of one order lower than the starting point. In general, the amount of enclosed modes appears to decrease for higher circumferential orders. In fact, investigations using higher order modes (not shown in this paper) have shown that, from a certain circumferential order, all corresponding radials describe closed and independent trajectories. Nevertheless, the mixed behavior observed on the first few radial orders in Figs. 3–5 remarks the importance of tracking the location of the eigenvalues as a function of frequency in order to correctly identify the ordering of the modes. For instance, other methods based on meshing the complex plane may provide the correct solution for a single frequency but they do not contain any information regarding the eigenvalue ordering. Finally, note that the hypothetical case of a double-pole solution, which depends on the particular impedance law, would occur when the trajectory of the bigger loop approaches one of the higher order modes. For those cases, a visualization like the ones presented in Figs. 3–5 can help identify any computation problem, which appears as a jump of the eigenvalues between trajectories. For most cases, a simple re-adjustment of the computation step or solving the equation starting from the liner anti-resonance (descending frequency) would fix the problem.

4.2. Axial wavenumbers

This section presents the axial wavenumbers k_z obtained from Eq. (7) in terms of the found eigenvalues k_{mn}. For simplicity, only the first circumferential order $m = 0$ is presented (the rest of the mode orders behave similarly). Fig. 6 presents the evolution of the computed wavenumbers in the complex plane as a function of

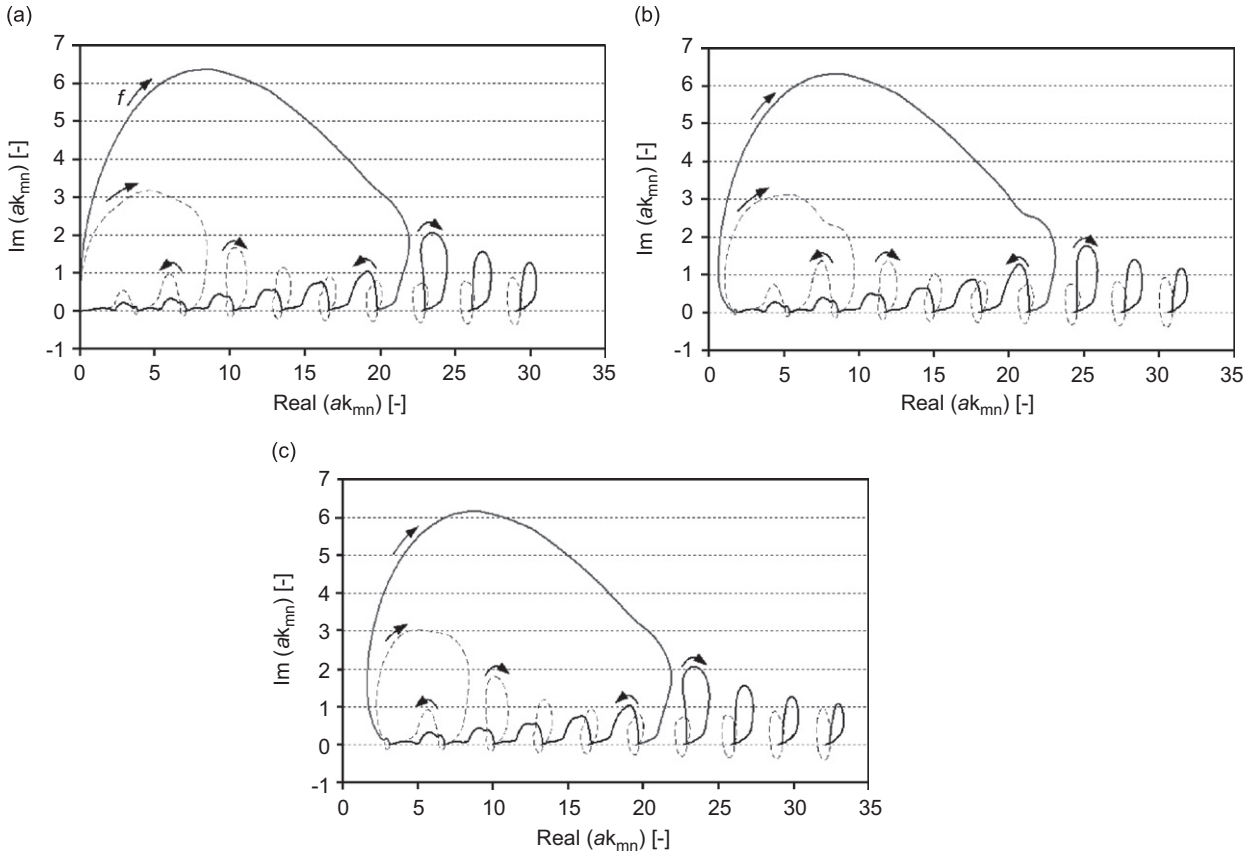

Fig. 5. Evolution of the non-dimensional eigenvalues in the complex plane for the circumferential mode orders: (a) $m = 0$, (b) $m = 1$ and (c) $m = 2$, including convective flow $M = -0.4$ and using the impedance law in Eq. (24). Key: (——) positive propagation eigenvalues $k_{mn}^{(+)}$ and (- - - - -) negative propagation eigenvalues $k_{mn}^{(-)}$.

frequency for the three flow conditions. As in the previous section, the first 10 radial orders are shown in the plots. The arrows indicate the direction of the evolution for increasing frequency. For very low frequency, the wavenumbers are located in proximity to the imaginary axis and, in fact, close to the hard wall wavenumbers. In addition, for high frequencies, the wavenumbers progress towards the real axis and, therefore, also approach the hard wall solutions. However, the transitional frequencies present a deviation produced mainly by the present liner, which causes the eigenvalues k_{mn} to become particularly different from the hard wall condition, e.g. the wavenumbers directly depend on k_{mn}. For the condition without flow, the solutions depart from the imaginary axis and move through the second or fourth quadrant of the complex plane, depending on the solution branch, to eventually reach the real axis at the higher frequencies. The solution branches in the second (dashed line) and fourth (solid line) quadrants directly correspond to negative and positive propagation, respectively. In contrast with the hard wall solution, the fact that the wavenumbers are located in the complex plane (rather than right on either axis) raises the concept of decaying modes instead of cut-on or cut-off modes. The decaying rate depends on the imaginary part of the wavenumber and the propagating component is given by the real part.

When flow is included in the simulations (Fig. 6(b) and (c)), the resulting wavenumbers are observed to be shifted towards the positive complex semi-plane. The main factor responsible for this shift is the real quantity $-k_0M/(1-M^2)$ in Eq. (7). Note that since the flow Mach numbers are negative, the effective shift is produced to the positive semi-plane. In all cases, the convergence to the real axis is observed to be quite smooth except for one order, which was identified to be the first radial mode. This mode shows a slight divergence away from

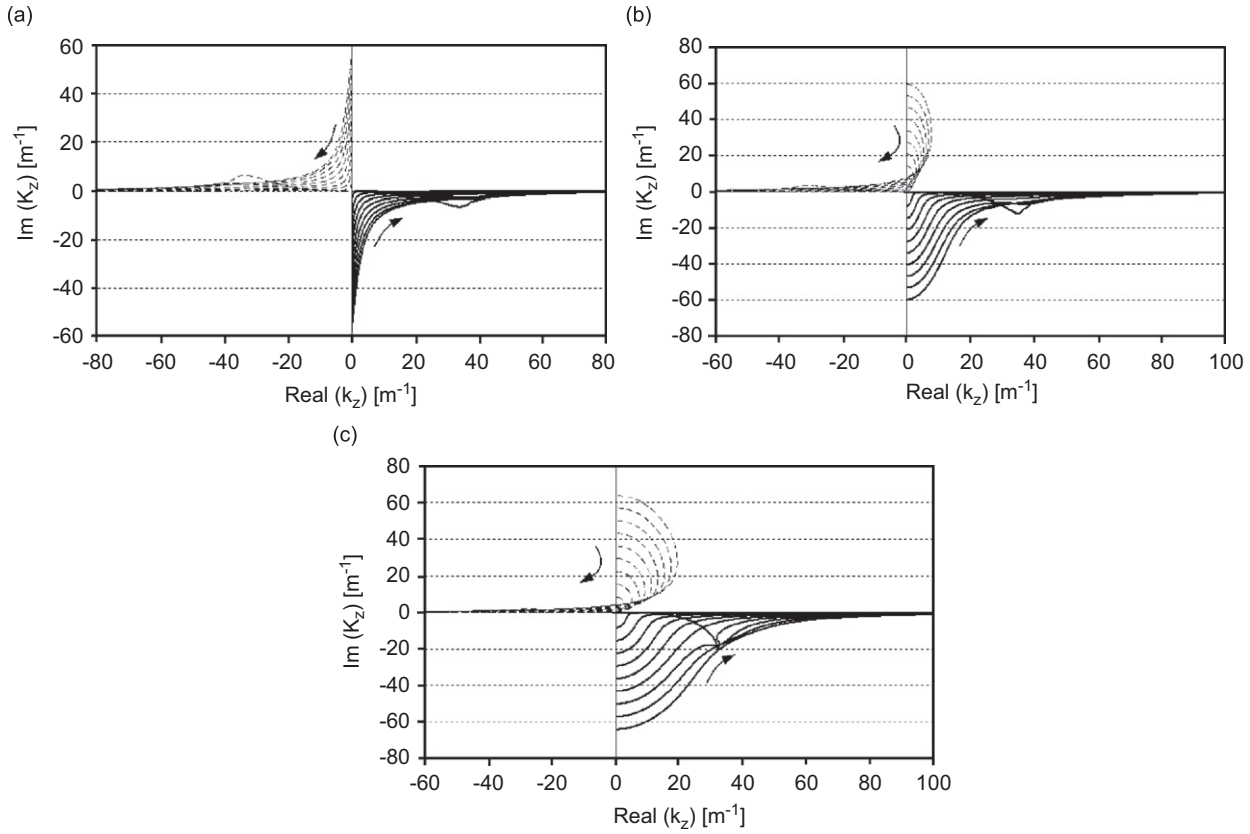

Fig. 6. Evolution of axial wavenumbers for the circumferential mode order $m = 0$ at flow Mach numbers: (a) $M = 0.0$, (b) $M = -0.2$, and (c) $M = -0.4$. Key: (——) positive propagation wavenumbers $k_{mn}^{(+)}$; and (- - - - -) negative propagation wavenumbers $k_{mn}^{(-)}$.

the real axis and then converges normally for high frequencies. This behavior can be explained due to the wide trajectory described by the corresponding eigenvalue that directly affects the square root term in Eq. (7). In order to see this effect in more detail, the results for the flow condition $M = -0.4$ were zoomed and are presented in Fig. 7. The highlighted (darker) curves for both propagating directions confirm the observation about the first radial order trajectory, i.e. for $n = 0$. The imaginary component that results from this deviation provides a significant attenuation rate causing the first radial mode not to be the least attenuated as it might be expected [3]. Furthermore, the convergence to the real axis of this first radial order for higher frequencies is surrounded by trajectories of two higher order modes. Therefore, the mode will not behave as the first radial order for high frequencies, but as some other mode of higher order. This result is directly related to the observed high-frequency trajectories of the eigenvalues k_{mn} in Figs. 3–5, where the first radial orders approach the hard wall eigenvalues of the last enclosed modes. In this particular case, these mode orders are $n = 6$ for positive propagating direction and $n = 2$ for negative direction, which exactly matches the trends in Fig. 5 for $M = -0.4$.

5. Final remarks

A numerical approach was applied to find the eigenvalues for the wave equation in a circular duct with soft wall boundary condition and convective uniform flow. This is very suitable for computing the mode attenuation properties of resonator-type liners commonly used in the aviation industry. The characteristic equation was derived in terms of the acoustic admittance of the wall in order to show the two possible solution branches depending on the direction of propagation. The final expression depends on the flow Mach number,

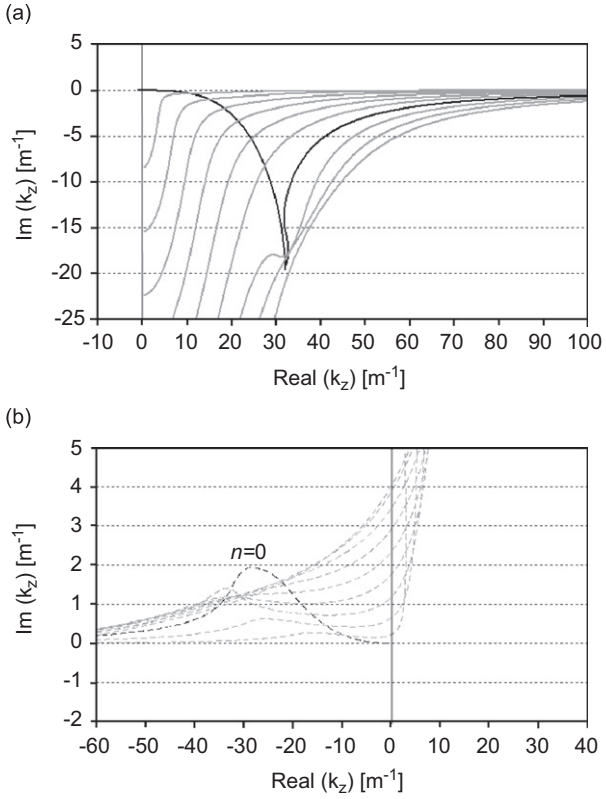

Fig. 7. Detailed trajectories of the axial wavenumber for the circumferential mode order $m = 0$ at flow Mach number $M = -0.4$: (a) positive propagation and (b) negative propagation. As $f \to \infty$, the first radial mode order in the lined condition approaches a higher radial order in an equivalent hard wall condition ($n_{HW} = 6$ for positive propagation and $n_{HW} = 2$ for negative propagation).

which couples the eigenvalues with the axial propagation constants (wavenumbers). Additionally, the resulting characteristic equations were found to be complex valued and nonlinear with respect to the unknown eigenvalues k_{mn}. Instead of directly seeking the zeros of the equation using root-finding methods, a more efficient numerical technique for minimization of real-valued functions of multiple variables was applied, i.e. the Nelder–Mead simplex method. To this end, the eigenvalues were found by minimizing the absolute value of the characteristic equation and assuming the real and imaginary part of the solution as two independent real variables.

A few numerical examples were presented. It was observed that the eigenvalues describe trajectories in the complex plane as a function of frequency, which start at the location of the hard wall eigenvalues (on the real axis) and return to these solutions at the frequency of anti-resonance of the liner. However, not all eigenvalues describe closed trajectories. If fact, the eigenvalues for the first radial orders tend to describe a wider path that encloses the trajectory of a few higher order modes. Consequently, at the higher frequencies close to the anti-resonance of the liner, the trajectory of these first radial orders approaches the hard wall eigenvalue of the last enclosed mode (instead of returning to the starting point). Subsequently, each enclosed mode approaches the hard wall eigenvalue of one order less than the starting point. This behavior stresses the importance of tracking the location of the eigenvalues as a function of frequency in order to identify the correct mode ordering.

The solution of the axial propagation constants (wavenumbers) was also investigated. The solutions start close to the imaginary axis for low frequencies and move towards the real axis across mainly the second and fourth quadrants, depending on the direction of propagation. Their trajectories on the complex plane were identified to be directly related to the corresponding eigenvalue solutions.

References

[1] P.M. Morse, K.U. Ingard, *Theoretical Acoustics*, McGraw-Hill Book Company, New York, 1968.
[2] D.C. Pridmore-Brown, Sound propagation in fluid flowing through an attenuating duct, *Journal of Fluid Mechanics* 4 (1958) 393–406.
[3] S.H. Ko, Sound attenuation in a lined rectangular duct with flow and its application to the reduction of aircraft engine noise, *The Journal of the Acoustical Society of America* 50 (6) (1971) 1418–1432.
[4] B.J. Tester, The propagation and attenuation of sound in lined ducts containing uniform or 'plug' flow, *Journal of Sound and Vibration* 28 (1973) 151–203.
[5] S.H. Ko, Sound attenuation in acoustically lined circular ducts in the presence of uniform flow and shear flow, *Journal of Sound and Vibration* 22 (1972) 193–210.
[6] M.K. Myers, On the acoustic boundary condition in the presence of flow, *Journal of Sound and Vibration* 71 (3) (1980) 429–434.
[7] B.J. Tester, Some aspects of 'sound' attenuation in lined ducts containing inviscid mean flows with boundary layers, *Journal of Sound and Vibration* 28 (2) (1973) 217–245.
[8] W. Eversman, *Theoretical Models for Duct Acoustic Propagation and Radiation, Aeroacoustics of Flight Vehicles: Theory and Practice*, Vol. 2, NASA Reference Publication 1258, TR 90-3052, 1991, pp. 101–163.
[9] W.E. Zorumski, Acoustic theory of axisymmetric multisectioned ducts, NASA TR R-419, 1974.
[10] J.A. Drischler, Analytic studies of sound pressures inside the duct of ducted propellers, NASA TN D-6345, 1971.
[11] J.A. Nelder, R. Mead, A simplex method for function minimization, *The Computer Journal* 7 (1965) 308–313.
[12] J.C. Lagarias, J.A. Reeds, M.H. Wright, P.E. Wright, Convergence properties of the Nelder–Mead simplex method in low dimensions, *SIAM Journal on Optimization* 9 (1) (1998) 112–147.
[13] COMPAQ, IMSL® Fortran 90 MP Library, Visual Numerics, Inc., 1999.
[14] W.H. Press, B.P. Flannery, S.A. Teukolsky, W.T. Vettering, *Numerical Recipes in C*, Cambridge University Press, Cambridge, UK, 1988.
[15] MATH WORKS, MATLAB, The Math Works, Natick, MA, 1994.
[16] R.F. Hallez, Investigation of the Herschel-Quincke Tube Concept as a Noise Control Device for Turbofan Engines, MS Thesis, Virginia Tech, 2001.
[17] S.W. Rienstra, A classification of duct modes based on surface waves, *Wave Motion* 37 (2003) 119–135.
[18] L. Rayleigh, *Theory of Sound*, Vol. 2, Dover Publications, New York, 1877 (re-issued 1945).
[19] J.W. Miles, On the disturbed motion of a plane vortex sheet, *Journal of Fluid Mechanics* 4 (5) (1958) 538–552.
[20] A.B. Friedland, A.D. Pierce, Reflection of acoustic pulses from stable and unstable interfaces between moving fluids, *Physics of Fluids* 12 (6) (1969) 1148–1159.
[21] K.W. Tam, Directional acoustic radiation from a supersonic jet generated by shear layer instability, *Journal of Fluid Mechanics* 46 (4) (1971) 757–768.
[22] S.W. Rienstra, Hydrodynamic instabilities and surface waves in a flow over an impedance wall, *Proceedings of the IUTAM Symposium on 'Aero- and Hydro-Acoustics'*, Springer, Heidelberg, 1985, pp. 483–490.
[23] D.T. Sawdy, R.J. Beckemeyer, J.D. Patterson, Analytical and experimental studies of an optimum multisegment phased liner noise suppression concept, NASA CR-134960, 1976.
[24] R.E. Kraft, Theory and Measurement of Acoustic Wave Propagation in Multi-segmented Rectangular Flow-ducts, PhD Dissertation, University of Cincinnati, 1976.
[25] W. Koch, W. Möhring, Eigensolutions for liners in uniform mean flow ducts, *AIAA Journal* 21 (2) (1983) 200–212.